In situ Transmission Electron Microscopy Observations of Sublimation in Silver Nanoparticles

Michael A. Asoro,[†] Desiderio Kovar,[†,‡] and Paulo J. Ferreira[†,‡,*]

[†]Materials Science and Engineering Program and [‡]Department of Mechanical Engineering, University of Texas at Austin, Austin, Texas 78712, United States

ABSTRACT *In situ* heating experiments were performed in a transmission electron microscope (TEM) to monitor the thermal stability of silver nanoparticles. The sublimation kinetics from isothermal experiments on individual nanoparticles was used to assess the actual temperatures of the nanoparticles by considering the localized heating from the electron beam. For isolated nanoparticles, beam heating under normal TEM operating conditions was found to increase the temperature by tens of degrees. For nominally isothermal experiments, the observed sublimation temperatures generally decreased with decreasing particle size, in agreement with the predictions from the Kelvin equation. However, sublimation of smaller nanoparticles was often observed to occur in discrete steps, which led to faceting of the nanoparticles. This discrete behavior differs from that predicted by conventional theory as well as from experimental observations in larger nanoparticles where sublimation was continuous. A hypothesis that explains the mechanism for this size-dependent behavior is proposed.

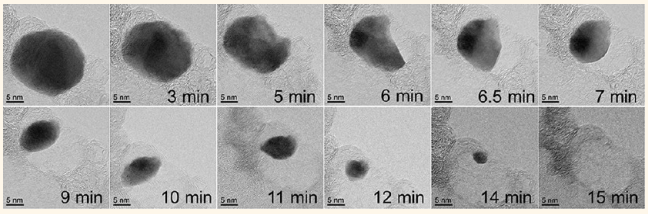

KEYWORDS: *in situ* transmission electron microscopy · nanoparticles · sublimation · kinetics · silver

Nanoparticles possess many unique properties that are distinct from that of bulk materials, which allows them to be used in applications such as in catalysis and in optical, magnetic and electronic devices. In particular, the thermal behavior of nanoparticles is expected to be different from that of bulk materials and may cause problems in applications where the particles experience elevated temperatures. For example, the melting temperature of nanoparticles has been shown to decrease with decreasing particle size.[1−7] Also, the temperature at which nanoparticles undergo direct sublimation without melting, as is the case for silver, or melting followed by evaporation, as is the case for gold, is depressed relative to bulk materials. This is critical for many sublimation-based purification processes, sublimation/condensation synthesis methods for producing nanomaterials and high temperature sintering processes of nanoparticles.

The particle size dependence on the kinetics of evaporation and sublimation can be predicted from bulk thermodynamics using the Kelvin equation and kinetic theory.[8,9] For the case of silver, this theory predicts a nearly constant sublimation rate until the particle size is reduced below about 20 nm, at which point the rate begins to increase significantly.

To determine if the Kelvin equation predicts the behavior of small particles, *in situ* transmission electron microscopy heating experiments were conducted to measure evaporation and sublimation rates.[9] This technique is essential to understand the sublimation process of nanoparticles, as it allows real-time direct measurements of the kinetics of sublimation which is not possible using post-mortem characterization. The aforementioned *in situ* transmission electron microscopy experiments were conducted with a miniature furnace that utilized a heating coil to indirectly heat the sample while a thermocouple was attached to the holder to monitor the temperature. The experiments confirmed the validity of Kelvin equation for silver particles larger than about 20 nm, where the sublimation rate is nearly constant but data below this size range, where the size effects are far more pronounced, were difficult to obtain

* Address correspondence to ferreira@mail.utexas.edu.

Received for review June 2, 2013 and accepted August 13, 2013.

Published online August 13, 2013
10.1021/nn402771j

because the resolution of the TEMs available at the time made it difficult to accurately measure smaller particle sizes. Moreover, the use of the conventional heating holders discussed above required relatively long times to equilibrate, which made it difficult to measure the faster sublimation rates that smaller particles exhibit. Thus, the validity of the Kelvin equation for small nanoparticles (<20 nm) has not been demonstrated. Moreover, while the Kelvin equation predicts a monotonic decrease with particle size, recent *in situ* transmission electron microscopy observations[10,11] suggest that small NPs facet and sublimate in discrete steps rather than continuously. This phenomenon needs to be explained.

In this work, we report the results of *in situ* transmission electron microscopy heating of silver nanoparticles using a novel heating stage that exhibits negligible thermal drift and allows very rapid heating rates. This allows the kinetics of sublimation to be measured during isothermal annealing by directly observing sublimation in small silver nanoparticles and to compare these results to those predicted by the Kelvin equation. This paper also addresses the most critical experimental challenge, which is accounting for the effects of beam heating on the actual temperature of particles in this size range. Note that this effect is particularly significant for modern TEMs with higher brightness guns that can result in very high beam fluxes. Lastly, we explore the causes of the nonmonotonic sublimation behavior that has been reported previously in small and faceted nanoparticles.[10,11]

Kinetics of Sublimation of Nanoparticles. The sublimation behavior of silver nanoparticles using *in situ* transmission electron microscopy[9−11] and the rate dependence on particle size have been studied previously. Following the derivation of Sambles *et al.*,[9] the Kelvin equation for a solid particle at equilibrium, is given by

$$\ln\frac{P_r}{P_\infty} = \left(\frac{M_r}{TR\rho}\right)\left(\frac{2\gamma}{r}\right) \tag{1}$$

where M_r is the molecular weight, R is the gas constant, ρ is the density of the solid, T is the temperature, P_r is the vapor pressure above a particle of radius r, P_∞ is equilibrium vapor pressure of the sublimating species over a flat surface, and γ is the surface energy of the solid assuming that it is isotropic. The rate of change of the particle radius with time, dr/dt, can be related to the number of molecules leaving the surface per unit time, n_v

$$\frac{dr}{dt} = n_v V_a \tag{2}$$

where V_a is the molecular volume. Utilizing kinetic theory, which gives the number of molecules of the vapor colliding with unit area of the particle surface per unit time, n_c, at equilibrium

$$n_v = \alpha n_c = \frac{1}{4}\alpha n\left(\frac{8RT}{\pi M_r}\right)^{1/2} \tag{3}$$

where α is the sticking coefficient for molecules arriving at the surface (assumed to be independent of particle radius) and n is the number of molecules in the vapor. Substituting eq 3, into eq 2 and assuming the vapor behaves as a monotonic perfect gas

$$\left.\frac{dr}{dt}\right|_r = \left(\frac{M_r}{2\pi R\rho^2}\right)^{1/2}\frac{\alpha P_r}{T^{1/2}} \tag{4a}$$

and

$$\left.\frac{dr}{dt}\right|_\infty = \left(\frac{M_r}{2\pi R\rho^2}\right)^{1/2}\frac{\alpha P_\infty}{T^{1/2}} \tag{4b}$$

Substituting eq 1 into eqs 4a and 4b and integrating while holding temperature constant, we obtain the time, t, to sublimate a particle, which is given by

$$t = \frac{B}{A}\left\{E_0\left(\frac{B}{r}\right) - E_1\left(\frac{B}{r}\right)\right\} \tag{5}$$

where the constants A, B, $E_0(x)$ and $E_1(x)$ are defined as

$$A = \alpha\left(\frac{M_r}{2\pi R\rho^2}\right)^{1/2}\frac{P_\infty}{T^{1/2}} \tag{6}$$

$$B = \frac{2M_r\gamma}{\rho RT} \tag{7}$$

$$E_0(x) = \frac{\exp(-x)}{x} \tag{8}$$

$$E_1(x) = \int_x^\infty \frac{\exp(-y)}{y}\,dy \tag{9}$$

Thus, using eq 5 and the materials constants expressed through eqs 7−9, it is possible to predict the particle radius, r, as a function of time, t, during an isothermal sublimation experiment.

***In situ* Transmission Electron Microscopy Sublimation of Nanoparticles: Critical Requirements.** *Heating Holder.* To address the issues discussed in the introduction, *in situ* heating experiments were performed in a TEM (JEOL 2010F) equipped with an Aduro heating stage[12] (Protochips Inc., Raleigh, NC). The heating stage uses a disposable, micro-electromechanical system (MEMS) device that serves both as the specimen support grid and the heating element by connecting the stage using electrical feed-throughs to an external power supply (Figure 1a). The MEMS device is a 150 nm thick, 500 × 500 μm, free-standing membrane made from a conductive ceramic that is suspended on a 4 × 6 mm silicon chip. For electron transparency, the ceramic membrane is patterned with a series of 6 μm diameter holes, which are subsequently overlaid with a holey carbon film, and which support the silver nanoparticles (Figure 1b,c). Joule heating occurs when electrical current is forced through the ceramic membrane, and this current is used to control the temperature. The current *versus* temperature response of the

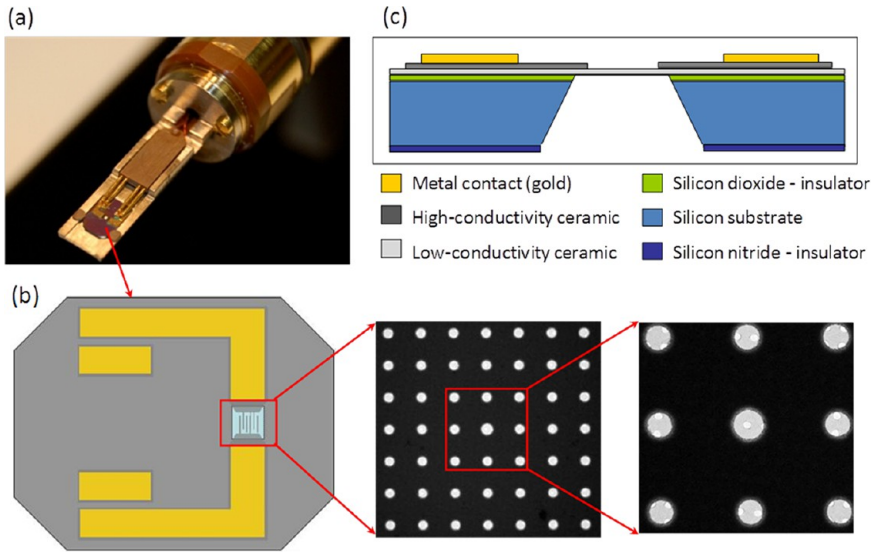

Figure 1. (a) Tip of specimen holder showing the heater chip clamped into place, with electrical leads connected. (b) Top view schematic of the heater chip. The insets are low-magnification TEM images of the central region of the chip showing the pattern of holes in the low-conductivity ceramic membrane and holey carbon support film overlaying the holes in the ceramic membrane. (c) Cross-section view of the chip shown in (b). (Courtesy of Protochips Inc.).

heating device is calibrated at the factory using an imaging pyrometer in a vacuum probe station (at a pressure similar to what is used in a TEM column). Unlike conventional heating holders, the low mass of this heating stage enables very fast heating rates (up to 10^6 °C/s) with extremely low thermal drift, even at high temperatures. This allows for isothermal experiments to be carried out in the TEM at high magnifications on very small particles, since the desired temperatures can be achieved nearly instantaneously.

Temperature Calibration for Nanoparticles. Because of the strong dependence of sublimation rate on particle size, the actual temperature experienced by larger (>20 nm) nanoparticles in a TEM can be accurately determined by monitoring the kinetics of the sublimation at a particular temperature and measuring the change of particle radius with time, as described by eq 5. Figure 2 shows a plot of particle radius with time from an isothermal experiment on a 28 nm nanoparticle at 600 °C. The experiment is compared to theoretical predictions for particles of the same size and at the same temperature. It is apparent that there is a discrepancy between the experimentally determined rate of sublimation and that predicted from theory. Since it is possible that some of the parameters used to determine the theoretical predictions, such as the surface energy, could exhibit a temperature dependence, the predictions were recalculated using plausible ranges for these parameters, but the experimentally measured curvature could not be replicated by varying only these parameters. An alternative hypothesis is that there was a discrepancy between the actual temperature experienced by the particles and the temperature of the heating stage. The solid line in Figure 2 shows that if the apparent temperature was

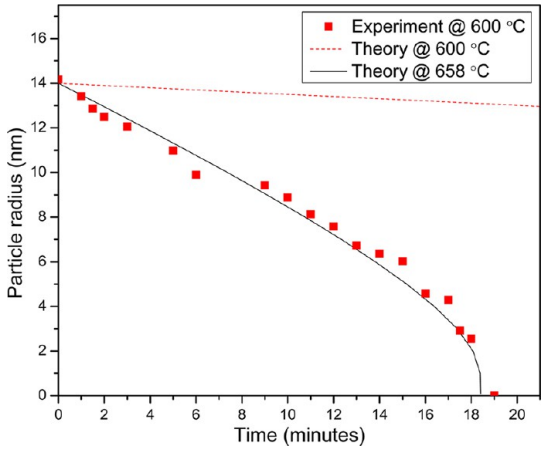

Figure 2. Particle radius *versus* time during an isothermal heating experiment at a nominal temperature of 600 °C on a 28 nm nanoparticle, based on the value displayed by the holder. The dashed and solid lines are the theoretical predictions calculated from eq 5 at 600 and 658 °C, respectively. These results suggest that the effective temperature is about 58 °C higher than indicated by the heating holder.

assumed to be 58 °C higher than that temperature indicated by the heating stage, a good match exists between the experiments and theory over the full range of particles sizes that were measured, from 28 nm to <6 nm. We have observed similar discrepancies in other experiments that can also be explained by temperature discrepancies of between 20 and 150 °C. As discussed in the section that follows, these discrepancies likely result primarily from beam-induced effects.

Beam Heating Measurements and Calculations. The nominal temperature of the heating stage only accounts for resistive heating of the specimen holder from the power supply, not the effects of heating from

the electron beam. Calculations by Hobbs[13] suggest that for metallic thin-film TEM specimens that have high conductivity, beam heating is negligible under standard TEM conditions. However, Gryaznov *et al.*[14] have shown that the temperature of isolated nanoparticles residing on a substrate can increase by as much as several hundred degrees under electron beam irradiation in the TEM because the contact area between the particle and the substrate is usually much smaller than the nanoparticle cross section. This restricted heat flux through the contact results in an increase in the average temperature in the nanoparticle compared to the substrate. The predicted magnitude of beam heating depends on contact geometry between the particle and the substrate, the intensity of the beam, and the size of the nanoparticles. In general, beam heating decreases with an increase in the contact angle or particle size and a decrease in current density. For a given beam current density, the temperature increase on the nanoparticle was shown to be proportional to the square of the particle radius.

The total beam current in our microscope, measured with a Faraday cup holder, was 4.565 nA, and the current density was determined to be about 4×10^4 A/m^2, which converts to 2500 electrons/Å^2. Using the model of Gryaznov *et al.*,[14] an equilibrium contact angle of about 8° was predicted for a 28 nm nanoparticle,[15] like that shown in Figure 2. For this combination of parameters, the temperature increase from beam heating as a function of particle size was calculated from the model and is shown in Figure 3. Because the actual contact angle is difficult to measure accurately in a TEM, the predicted beam heating for contact angles of 0 and 3° is also shown to illustrate the range of behaviors that are possible for contact angles <8°. Note that the predicted beam heating is not sensitive to contact angle for large contact angles, and thus the beam heating effects for larger contact angles would not vary significantly from that predicted for 8°. The plot shows that for a 28 nm nanoparticle, observed under typical operating conditions, the predicted temperature increase from beam heating is about 90 °C. This is greater than the 58 °C discrepancy between the heating stage temperature and the temperature that was determined from the sublimation experiment, assuming the contact angle was 8°. However, it is within the predicted range given the uncertainties in the contact angle.

These experiments show that beam heating effects during *in situ* heating of nanoparticles can lead to temperature discrepancies between the actual and nominal temperature of the heating stage of at least many tens of degrees in very small particles. Since the discrepancies will vary for particles even in the same field of view due to differences in contact with the substrate, the uncertainty in the actual temperature should be considered carefully when quantitatively assessing the kinetics of processes such as sublimation. These effects will also vary depending on the imaging conditions (beam size) and the intensity of the electron source used in the TEM. Additional errors in temperature may exist from the calibration of the TEM specimen holder, since this calibration is typically performed independently of other measurements. Recently, the manufacturer revised the calibration procedure so it no longer uses extrapolation at temperatures below 600 °C and therefore is much more accurate for temperatures of 400−600 °C.

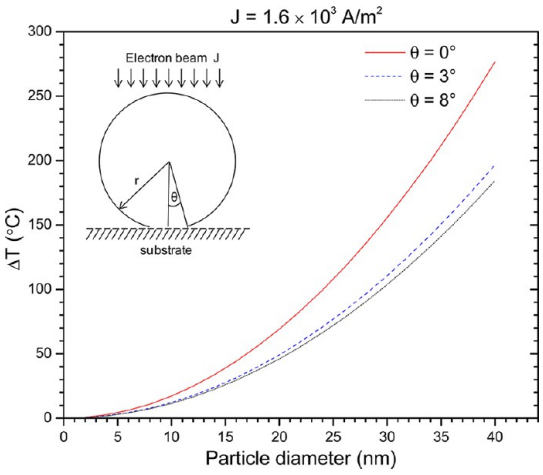

Figure 3. Temperature increase *versus* particle diameter due to electron beam heating. The inset is a schematic of a nanoparticle of radius, *r*, under an electron beam with current density, *J*, and contact angle with substrate, θ.

RESULTS AND DISCUSSION

A sequence showing selected TEM images of silver nanoparticles at room temperature and during *in situ* transmission electron microscopy heating at stage temperatures ranging from 500 to 720 °C in increments of 10 °C is shown in Figure 4. Note that the nanoparticles labeled A−K shrink in size, vanish from the support (represented by the red empty circles in the TEM images), or remain stable depending on the nanoparticle size and temperature. The stage temperature at which the nanoparticles begin to shrink generally decreases with decreasing particle size as seen in Figure 5a,b. However, some exceptions are also apparent which suggests that the actual temperature varies from particle-to-particle (see, for example, particles D and E in Figures 4 and 5a) due to the beam heating effects that were discussed previously.

An experiment was conducted at high magnification (see Figure 6a,b) on a 20 nm nanoparticle at a stage temperature of 580 °C for 15 min to study the mechanism of sublimation. The nanoparticle size decreases as time progresses, and as the particle continues to shrink, facets become apparent (Figure 6a). A more detailed bright-field TEM image of the nanoparticle shows clearly that during the isothermal heating experiment, lattice fringes are present even up to the

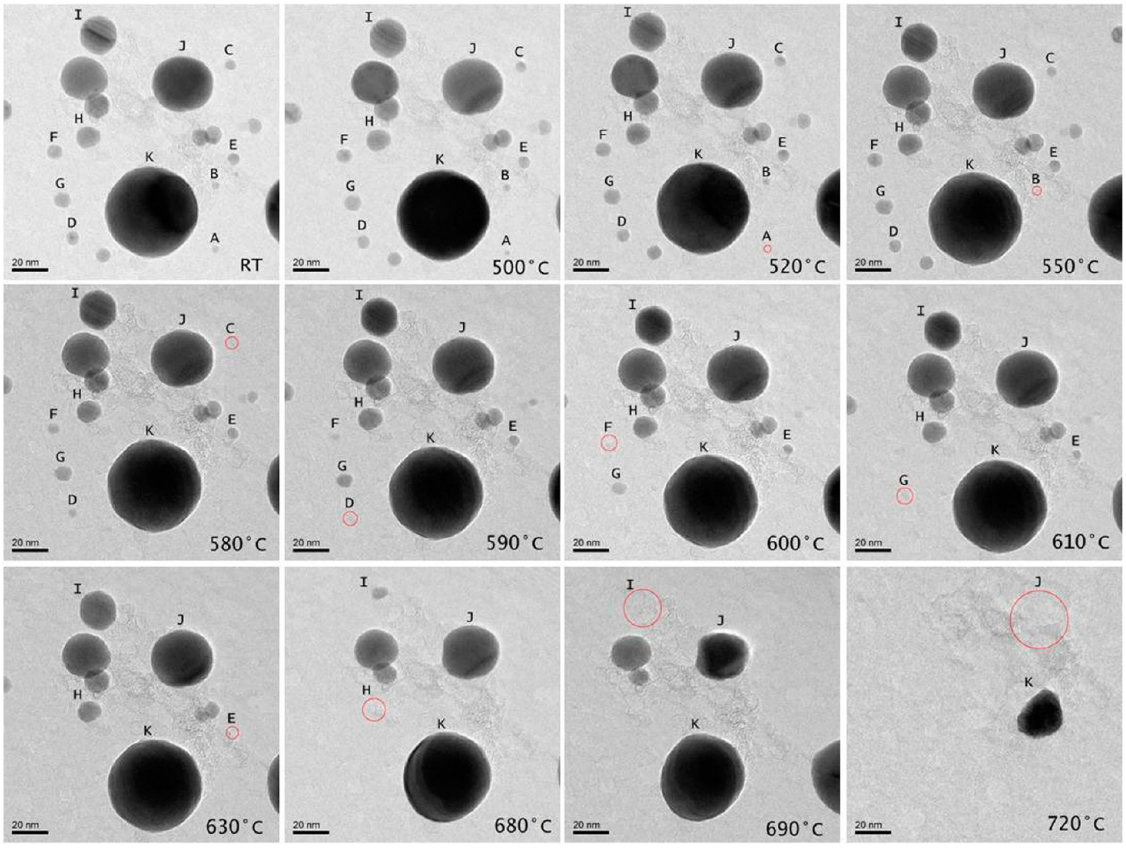

Figure 4. Selected bright-field TEM images of silver nanoparticles at room temperature (RT) and at temperatures ranging from 500 to 720 °C.

edge of the nanoparticle (Figure 6b), indicating that the nanoparticle remains crystalline while shrinking. Since no amorphous material is present that would be indicative of the presence of a liquid on the particle surface, this confirms that silver nanoparticles transform directly from the solid to the vapor phase by sublimation.

The sublimation temperatures were recorded as the temperatures at which the particle first started to shrink. Figure 7 shows the sublimation temperatures for a number of nanoparticles with different initial sizes. Smaller nanoparticles generally sublimate at lower temperatures, as expected. The size-dependent melting temperature calculated from theory[16] is also included for comparison, and it is apparent that sublimation occurs at much lower temperatures than the expected melting temperature.

For the larger nanoparticles, the particles shrink while remaining spherical. In contrast, many of the smaller nanoparticles form distinct facets, and the sublimation process occurs in bursts rather than continuously (see movie file in the Supporting Information). The fast Fourier transforms (FFTs) of the images in Figure 6a allow us to determine the crystallographic orientation of the facets which seem to form on low index {100} and {111} planes. This nonmonotonic sublimation mechanism has been reported previously in silver nanocubes[11] and was attributed to the strong adhesion of the surfaces of the cube with the carbon capping shell.

To better understand the noncontinuous sublimation behavior that we observed in smaller nanoparticles, we present a simple analytical model to calculate the energetics of sublimation for particles that sublimate uniformly and compare this energy to that required for sublimation *via* a noncontinuous faceting mechanism. Details of this model are presented in the Supporting Information. We consider two possible mechanisms for sublimation, as shown in Figure 8. In route 1, the particle shrinks from a size r_1 to r_2 by a solid-to-vapor transition that uniformly removes solid from the particle surface. In route 2, the particle first splits into two faceted particles, before the smaller particle is assumed to quickly sublimate. This process may be favored if the surface energy of the facet is considerably lower than the mean surface energy for a spherical particle. For either process, we assume that the starting and ending volumes of the particles are the same.

For the uniform sublimation mechanism (route 1), we consider the changes in energy that occur during sublimation. These include the total surface energy of the particles, the volume free energy of the solid particles, and the volume free energy of the vapor that

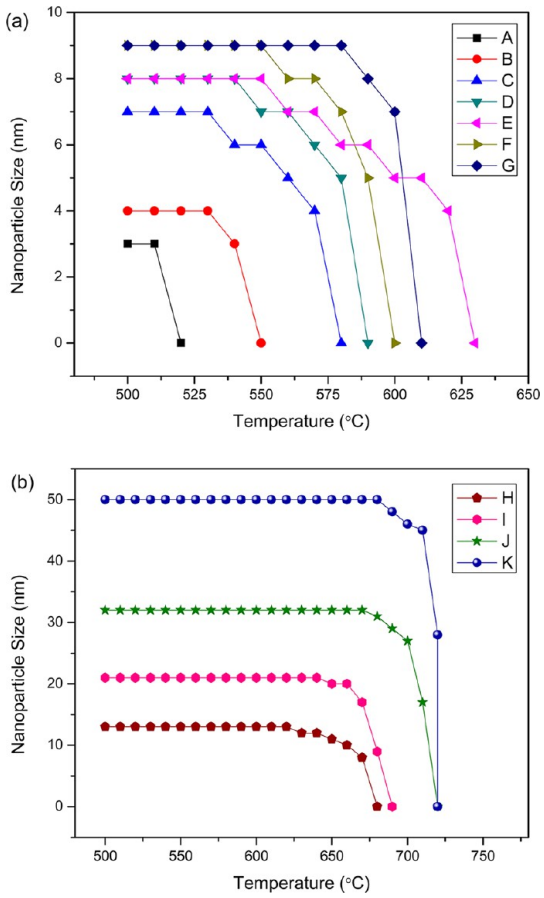

Figure 5. Nanoparticle size as a function of temperature for particles labeled (a) A–G (b) H–K in Figure 4.

is sublimated. The total change in energy upon uniform sublimation is given by

$$\Delta E_u = \{4\pi\gamma_s(r_2^2 - r_1^2) + 4/3\pi E_{sub}(r_2^3 - r_1^3) \quad (10)$$

where $r_2 = [r_1^3 - 3/4(r_1 x^2 - x^3/(4\pi))]^{1/3}$, γ_s is the surface energy per unit area and E_{sub} is the heat of sublimation. For the case of the nonuniform sublimation (route 2), we consider the surface energy of the larger faceted particle, the volume energy of the larger faceted particle, and the volume energy of the smaller faceted particle (which consists of vapor after sublimation and therefore has no interfacial area). The total change in energy for nonuniform sublimation is therefore given by

$$\Delta E_f = \pi\gamma_{s111}(2r_1 x - x^2) - 2\pi\gamma_s r_1 x + E_{sub}\left(\frac{\pi x^3}{3} - \pi r_1 x^2\right) \quad (11)$$

where γ_{s111} is the surface energy of the low energy $\{111\}$ plane formed upon faceting. If faceting occurs at twin boundaries, the twin energy should be used but based on observations, such as Figure 6, faceting does not occur exclusively at twin boundaries, and we therefore did not include this energy since it does not affect ΔE_f.

Figure 9a shows the differences in the change in energies ($\Delta E_u - \Delta E_f$) for sublimation by nonuniform and uniform mechanisms calculated from eqs 10 and 11 as a function of the initial particle size r_1. Since the changes in energy ΔE_u and ΔE_f are both negative, if

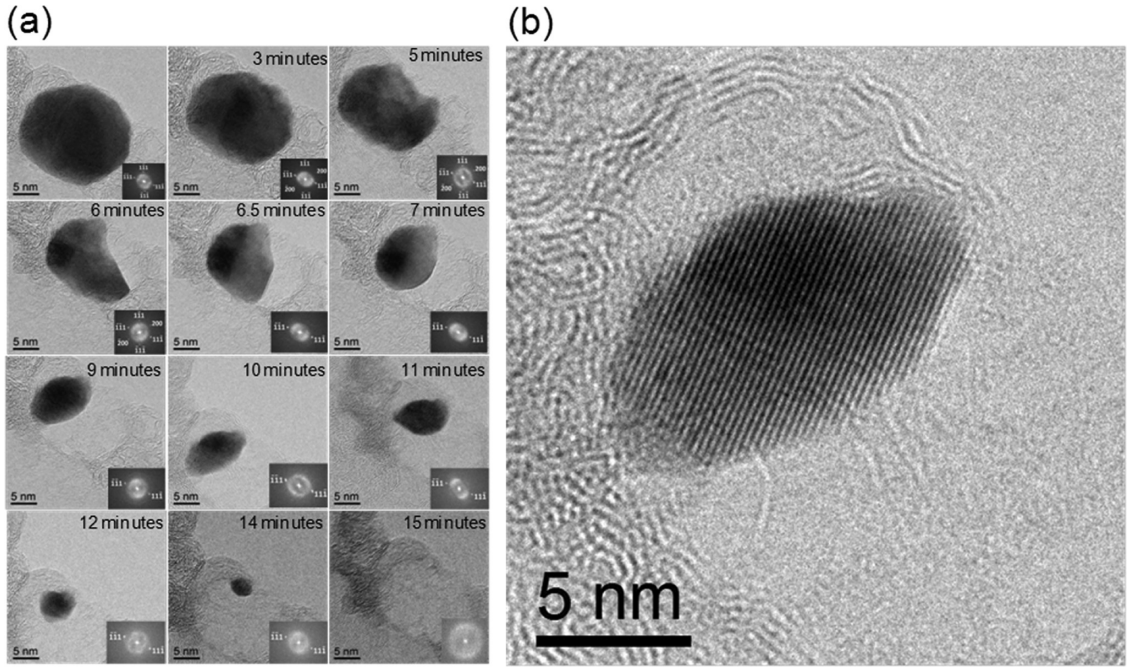

Figure 6. (a) Sequence of TEM images during an isothermal experiment at 580 °C, showing the sublimation of a 20 nm silver nanoparticle. The insets are the FFTs of the TEM images. (b) High-resolution TEM image of the silver nanoparticle in (a) after 10 min. The lattice fringes indicate that the nanoparticle remains solid and crystalline during sublimation.

$\Delta E_u - \Delta E_f$ is positive, then the magnitude of the energy change for uniform sublimation is lower than for nonuniform sublimation. Thus, when $\Delta E_u - \Delta E_f$ is positive, nonuniform sublimation is energetically favored. If on the other hand, $\Delta E_u - \Delta E_f$ is negative, then uniform sublimation is favored. Consider the case when nonuniform sublimation from a small facet ($x/r_1 = 0.07$) is compared to that for uniform sublimation for a large particle ($r_1 > 40$ nm). In this case $\Delta E_u - \Delta E_f$ is negative and uniform sublimation is therefore initially expected. As the particle size is decreased to about 30 nm, $\Delta E_u - \Delta E_f$ transitions from negative to positive. As the particle size is reduced further, the differences in energies, $\Delta E_u - \Delta E_f$, increase, reach a peak, and then decrease but remain positive for all values of r_1 less than about 30 nm. This indicates that for particles smaller than ~30 nm, small facets are favored, whereas for larger nanoparticles, uniform sublimation is favored. Similar trends are apparent when larger facets are considered ($x/r_1 = 0.08-0.25$). However, as the facet size is further increased, the particle size at which faceting would first be expected decreases.

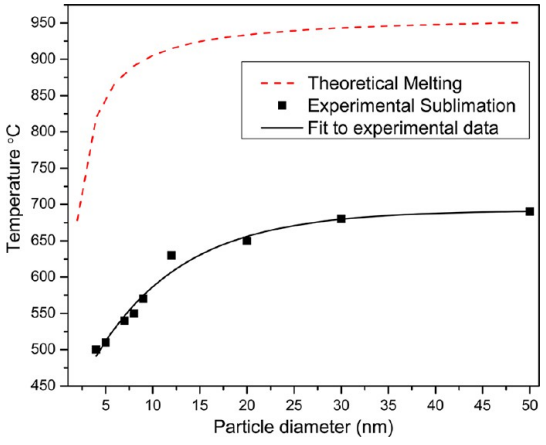

Figure 7. Experimentally observed sublimation temperature *versus* nanoparticle size, showing clearly that the theoretically calculated melting temperature as a function of nanoparticle size occurs at significantly higher temperatures than sublimation.

The dashed line in Figure 9a at $E_u - \Delta E_f = 0$ represents the boundary between uniform and nonuniform sublimation. For a given x/r_1, the largest radius at which nonuniform sublimation is energetically favored, r_{cr}, can be determined from the intersection of the curves with the dashed line. Note, however, that the energy difference between nonuniform and uniform sublimation continues to increase as the particle size is reduced below r_{cr} and reaches a peak before decreasing again. The particle radius at which the energy difference between uniform and nonuniform sublimation is maximized at this peak can therefore be considered to be the equilibrium radius at which that facet will form and is given the designation r_e. The normalized facet size, x/r_1, is plotted *versus* the initial particle size, r_1, in Figure 9b. The dashed line in this plot is r_{cr}, the largest particle size for which a facet of that size is energetically favored and is therefore metastable. The solid line is r_e, the equilibrium particle size determined from the peaks in the curves shown in Figure 9a and is the equilibrium particle size for a facet of that size. This plot shows that when the particle size is large, uniform sublimation is expected. As the

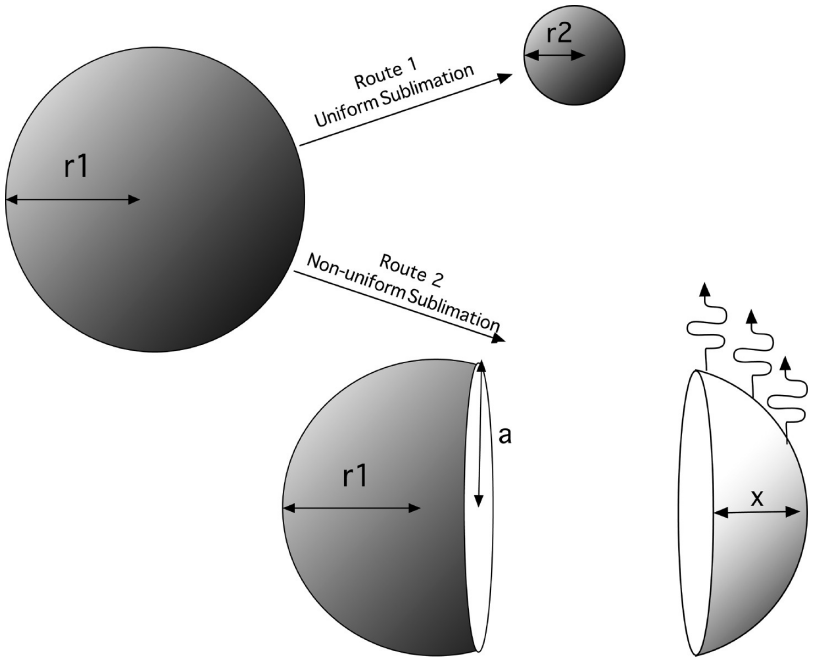

Figure 8. Two possible routes considered for sublimation of a nanoparticle of radius r_1. Route 1 assumes uniform sublimation, whereas route 2 assumes that the particle first splits into two faceted particles and then the smaller particle sublimates quickly.

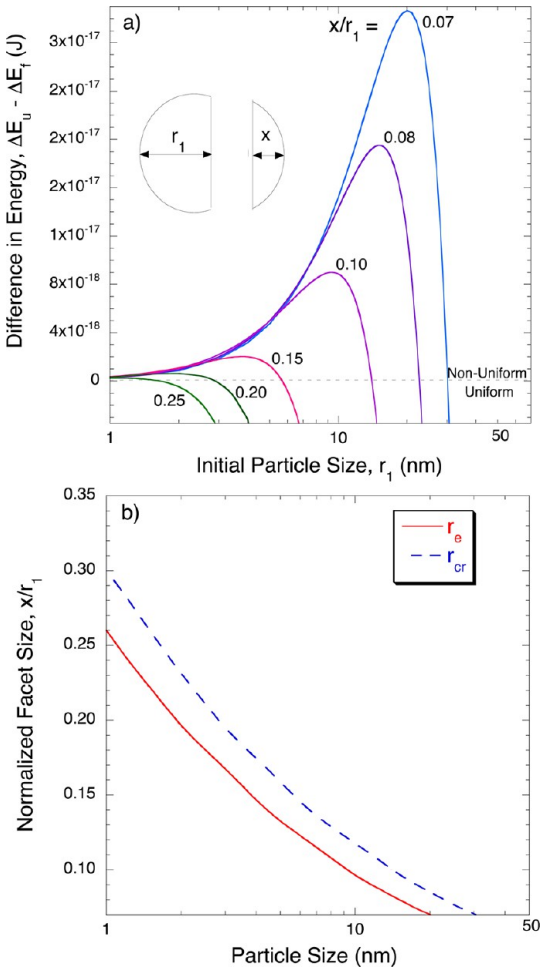

Figure 9. Difference in energy between the energy change for uniform and faceted sublimation *versus* particle size (a) and the predicted equilibrium (r_e) and critical (r_{cr}) facet size *versus* particle size (b).

particle size is reduced, very small facets are expected to form during sublimation. For example, facets with $x/r_1 = 0.08$ are expected only when the particle size is reduced below 20 nm. As the particle size is reduced further, the size of the facets increases sharply. For example, for $r_1 = 1$ nm, facets with $x/r_1 = 0.26$ are predicted.

Comparing our experiments to the model, good qualitative agreement is observed. For example, in the sequence of micrographs shown in Figure 6, the particle is initially nearly spherical and during the initial stages of sublimation remains nearly spherical. It is possible that small facets are forming at this stage, but in practice, it is difficult to distinguish between a particle that consists of very small facets and one that is spherical. After about 5 min at 580 °C, a large facet suddenly forms. As the particle continues to sublimate, it occurs by discrete changes in particle size rather than uniformly, and it is accompanied by the formation of large facets. In this series of images, the first large facet forms at $r_1 \approx 9$ nm at $x/r_1 \approx 0.22$. The model predicts for a particle of this size, the equilibrium facet size should be $x/r_1 \approx 0.10-0.13$. The lack of quantitative agreement between the experiment and model may arise from uncertainties in some of the thermodynamic values (like the surface energy and sublimation energy) that have been assumed in the model. Nevertheless, the qualitative agreement between this simple model and experiment provides insight into the possible transition from uniform sublimation when the particles are large to nonuniform sublimation accompanied by faceting when the particle size is small.

CONCLUSIONS

The actual temperature experienced by nanoparticles during *in situ* heating transmission electron microscopy experiments has been studied by observing sublimation of silver nanoparticles with diameters of 5−50 nm at temperatures of 500−700 °C. The kinetics of sublimation was monitored and revealed that the actual temperature experienced by the nanoparticles during *in situ* heating in a TEM were consistently higher than the indicated temperatures that were determined from independent calibrations. Calculations show that this discrepancy is likely the result of electron beam heating of the nanoparticles which can vary significantly from particle-to-particle, particularly due to variations in contact with the carbon support and variations in particle sizes. These results show that beam heating effects should be taken into account when performing *in situ* heating experiments on nanoparticles and provides a method for measuring the uncertainty in the temperature when conducting such experiments by monitoring the sublimation kinetics of larger nanoparticles. As predicted from theory, we observe that the sublimation temperatures of nanoparticles decrease with decreasing particle size in general agreement with the Kelvin equation. However, we also observed that for smaller nanoparticles, sublimation often occurs in discrete steps with faceting of the nanoparticles, whereas larger nanoparticles were observed to remain nearly spherical and sublimate continuously. We propose that differences in the total energy of the nanoparticle can explain this size dependence to the sublimation mechanism.

METHODS

Silver nanoparticles with a nominal size of 15 nm were obtained from NovaCentrix (Austin, TX). These nanoparticles were synthesized using a pulsed plasma, dry synthesis method in which a carbon source was added to the manufacturing process to minimize agglomeration of the nanoparticles. For observation in the TEM, as-received silver nanoparticles were first dispersed in deionized water and placed in a sonicator for

10 min to reduce particle aggregation. The suspension was then transferred onto an Aduro MEMS heating device. After the water was evaporated, the heating device was placed in a Protochips specimen holder for subsequent TEM observation.

The silver nanoparticles were heated *in situ*, first from room temperature to 500 °C. We did not observe any changes in the nanoparticles within this temperature range. Subsequently, the temperature was increased in increments of 10 °C from 500 to 720 °C and changes in the nanoparticles were monitored. TEM images were recorded *in situ* at each temperature. Later, isothermal heating experiments were carried out on individual nanoparticles to monitor the kinetics of sublimation. These experiments were performed using phase contrast imaging, so that lattice fringes, surface morphology and faceting could be clearly observed in the nanoparticles during the *in situ* heating experiments. Combining these observations provided insight into the mechanisms for sublimation.

Conflict of Interest: The authors declare no competing financial interest.

Acknowledgment. This work was supported by the National Science Foundation under DMR 1006894. We also wish to thank J. Damiano and S. Mick of Protochips Inc. for valuable discussions concerning the *in situ* transmission electron microscopy heating stage used for these experiments.

Supporting Information Available: Movie showing sublimation of silver nanoparticles and Appendix for derivation of faceting energy for nanoparticles. This material is available free of charge *via* the Internet at http://pubs.acs.org.

REFERENCES AND NOTES

1. Takagi, M. Electron-Diffraction Study of Liquid-Solid Transition of Thin Metal Films. *J. Phys. Soc. Jpn.* **1954**, *9*, 359–363.
2. Wronski, C. R. M. The Size Dependence of the Melting Point of Small Particles of Tin. *Br. J. Appl. Phys.* **1967**, *18*, 1731–1737.
3. Buffat, P.; Borel, J. P. Size Effect on the Melting Temperature of Gold Particles. *Phys. Rev. A* **1976**, *13*, 2287.
4. Blackman, M.; Curzon, A. E. On the Size Dependence of the Melting and Solidification Temperatures of Small Particles of Tin. *Struct. Prop. Thin Films* **1959**, 217.
5. Allen, G. L.; Bayles, R. A.; Gile, W. W.; Jesser, W. A. Small Particle Melting of Pure Metals. *Thin Solid Films* **1986**, *144*, 297–308.
6. Saka, H.; Nishikawa, Y.; Imura, T. Melting Temperature of In Particles Embedded in an Al Matrix. *Philos. Mag. A* **1988**, *57*, 895–906.
7. Wang, Z. L.; Petroski, J. M.; Green, T. C.; El-Sayed, M. A. Shape Transformation and Surface Melting of Cubic and Tetrahedral Platinum Nanocrystals. *J. Phys. Chem. B* **1998**, *102*, 6145–6151.
8. Sambles, J. R. Electron Microscope Study of Evaporating Gold Particles - Kelvin Equation for Liquid Gold and Lowering of Melting Point of Solid Gold Particles. *Proc. R. Soc. London, Ser. A* **1971**, *324*, 339–351.
9. Sambles, J. R.; Skinner, L. M.; Lisgarten, N. D. An Electron Microscope Study of Evaporating Small Particles - Kelvin Equation for Liquid Lead and Mean Surface Energy of Solid Silver. *Proc. R. Soc. London, Ser. A* **1970**, *318*, 507–522.
10. Lee, J. G.; Lee, J.; Tanaka, T.; Mori, H. *In situ* HREM Observation of Crystalline-to-Gas Transition in Nanometer-Sized Ag Particles. *Phys. Rev. Lett.* **2006**, *96*, 075504.
11. Ding, Y.; Fan, F. R.; Tian, Z. Q.; Wang, Z. L. Sublimation-Induced Shape Evolution of Silver Cubes. *Small* **2009**, *5*, 2812–2815.
12. Allard, L. F.; Bigelow, W. C.; Jose-Yacaman, M.; Nackashi, D. P.; Damiano, J.; Mick, S. E. A new MEMS-Based System for Ultra-High-Resolution Imaging at Elevated Temperatures. *Microsc. Res. Tech.* **2009**, *72*, 208–215.
13. Hobbs, L. W. *Introduction to Analytical Electron Microscopy*; Plenum Press: New York, 1979.
14. Gryaznov, V. G.; Kaprelov, A. M.; Belov, A. Y. Real Temperature of Nanoparticles in Electron Microscope Beams. *Philos. Mag. Lett.* **1991**, *63*, 275–279.
15. Johnson, K. L.; Kendall, K.; Roberts, A. D. Surface Energy and the Contact of Elastic Solids. *Proc. R. Soc. London, Ser. A* **1971**, *324*, 301–313.
16. Couchman, P. R.; Jesser, W. A. Thermodynamic Theory of Size Dependence of Melting Temperature in Metals. *Nature* **1977**, *269*, 481–483.